14th World Congress on Computational Mechanics (WCCM)
ECCOMAS Congress 2020)
Virtual Congress: 11-–15 January 2021
F. Chinesta, R. Abgrall, O. Allix and M. Kaliske (Eds)

STUDY ON THE EFFECTS OF ADDING DIAGONAL SPRINGS IN A RIGID BODY SPRING MODEL WITH QUADRILATERAL ELEMENTS

V. Tateo[1]

[1]Department of Architecture, Built environment and Construction engineering
Politecnico di Milano - Piazza Leonardo da Vinci 22, Milano
vito.tateo@polimi.it

Key words: Discrete models, Rigid Body Spring Model, Lattice models, Fracture energy, Poisson ratio, Failure anisotropy

Abstract. An improved Rigid Body-Spring model (RBSM) for in-plane analyses is here proposed. The approach has been developed starting from the model presented by Casolo [4], according to which a continuum plate is discretized in an assembly of rigid quadrilateral elements connected by elastic-plastic springs. In the proposed model, not only the elements that share one edge are connected, as it usually happens in RBSMs, but also the elements that share only one node, that are the elements on the diagonals. These elements are connected through an axial spring fixed to their centers of gravity. The spring stiffnesses have been obtained through the equivalence of the stored strain energy for a plane stress state. These, for an isotropic material, results to be function of the Young's modulus (E) and of the Poisson's ratio (ν). Thanks to the addition of the diagonal springs, this quadrilateral RBSM is capable of modeling isotropic materials with a Poisson's ratio different from zero. The effectiveness of the proposed computational method was proved comparing the elastic solution with a Finite element code for an uni-axial tensile test.
About the failure response, on one hand, the addition of the diagonal springs introduces a new direction in which the failure condition is verified, reducing the intrinsic anisotropy of the failure response, typical of the discrete approaches [5, 14]. On the other hand, the new springs increase the complexity of the model and the spring constitutive behavior is no longer directly related to the material uni-axial behavior. In this work, the spring post elastic response was defined considering the mode I fracture energy of the material. In the end, the model was applied to the study of a concrete notched beam in a three point bending test. The results have been compared with the experimental one find in the literature. The analyses were executed with a dynamic explicit solver and different tensile spring behaviors were compared to highlight the importance of considering a bi-linear softening law for modeling the failure response of quasi-brittle materials like concrete.

1 INTRODUCTION

Over the last decades many authors have developed discrete computational approaches for their capability of dealing with crack propagation problems, especially in brittle materials [2, 15, 4, 8]. They are all based on the same idea of discretizing a solid in particles interacting among them according to specific rules. An idea that was first developed by Hrennikoff [11] with a lattice model, but that has even more ancient origins in Navier's molecular model for solid mechanics [3]. If, on one hand, each discrete ap-

proach has been successfully and widely applied to some problems according to its peculiarities, on the other hand, some of them showed some limits especially dealing with isotropic materials. In fact, due to the discrete nature of the interactions and depending on the model topology some discrete approaches have an intrinsic fixed Poisson's ratio or show an isotropic elastic response only for a specific Poisson's ratio [19, 13]. This problem emerged already in the Navier's molecular model, that was characterized by only one constant, differently from what was suggested by the experimental evidence for the isotropic materials [3]. About the post-elastic response, according to the simplicity principle that characterize the discrete approaches, the failure criterion are usually bond based, i.e. the failure of the bond only depends on the bond state and stretch. This leads to an intrinsic anisotropy of the failure surfaces, that only the increase of the directions of interaction can reduce [12, 9, 14].
Among the discrete approaches the plane RBSM developed by Casolo [4] (RBSMc) was here investigated. This model is characterized by a simple mechanistic structure, with quadrilateral rigid elements interacting through normal and shear springs fixed on their sides. It has been widely applied to the study of a complex material like masonry [18, 7, 6], exploiting the possibility of defining a perfect correspondence between the spring constitutive behavior and the material uni-axial and shear responses, thanks to its simple mechanistic structure. But, even if the model has two independent constants (the normal and the shear spring stifnesses), it shows an isotropic elastic response only for materials with a null Poisson's coefficient, i.e. it has only one independent constant for isotropic materials, as observed in quadrilateral lattice models. Furthermore the limited number of interactions leads to a considerable anisotropy of the failure surfaces working with isotropic materials [5].
In this study, the effects, on the RBSM properties, of the addition of a new interaction between the elements on the diagonals are investigated. After the presentation of the new model topology (RBSMd), the model elastic parameters, i.e. the spring stiffnesses, were obtained and the model elastic response analyzed. Subsequently, the failure response of the new model was compared with the original one. In the end, the model was applied to the study of a mode I crack propagation problem in a concrete notched beam, comparing different tensile springs behaviors, to evaluate the model capability of dealing with failure analyses of isotropic quasi-brittle materials.

2 RBSM WITH DIAGONAL SPRINGS

In agreement with the RBSM proposed by Casolo, a lamina is discretized in n quadrilateral rigid elements, each i-element has 3 degrees of freedom (two displacements u_i, v_i, and one rotation ϕ_i) and the nodes of one element cannot be on the side of another one. Differently from the original model, the elements interact among them not only if they share one side, but also if they share only one node, i.e. if they are elements on the diagonals. The elements that share one side interact through four eccentric springs: two springs are parallel to the side, and will be called shear springs, and two springs are perpendicular to the side and will be called normal springs. Differently from the original model, in this case also the shear springs have been split, in order to have one shear spring for each normal spring, necessary for a coupled failure response. The eccentricity of the springs was defined in agreement with the indications of Casolo [4], but the influence of this parameter should be deepen in future studies. The elements on the diagonals interact only through one axial spring that connects their centers of gravity, these springs will be called diagonal springs. The fundamental cell of the model is composed by the four quarters of elements around a node and the springs that connect them (see Figure 1). This is the minimum entity of

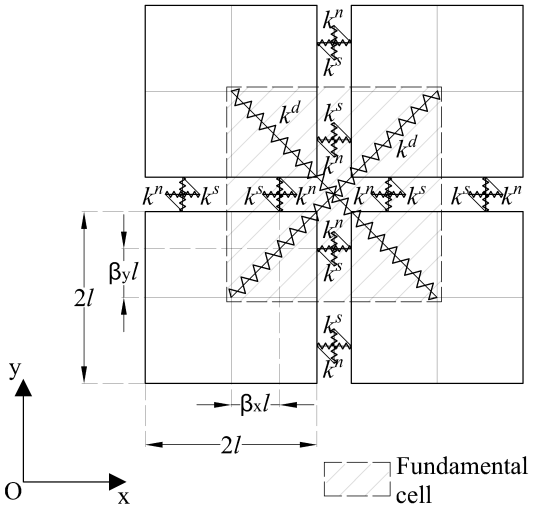

Figure 1: Fundamental cell of the rigid body spring model with diagonal springs (RBSMd)

the model that has to be considered to obtain the model parameters.
The spring state is defined in function of the average spring strain $\epsilon^{(b)}$. This is the ratio between the variation of the spring length, in the spring direction (in agreement with a small displacement theory), and the distance between the centers of gravity of the connected elements. The average spring strain is related to the problem degrees of freedom (collected in the vector U) through the $[B]$ matrix:

$$\{\epsilon\} = [B]U \tag{1}$$

The elastic strain energy associated to any spring has the form:

$$U^{(b)} = \frac{1}{2}\,\epsilon^{(b)^2}\,k^{(b)}V^{(b)} \tag{2}$$

where: $k^{(b)}$ is the spring modulus and $V^{(b)}$ is the volume of pertinence of the spring, that is equal to the sum of the two quarters of the elements connected by the spring.
The model elastic stiffness matrix is so computed as:

$$[K] = [B]^T[k][V][B] \tag{3}$$

where: $[k]$ is a diagonal matrix of the spring moduli and $[V]$ is the diagonal matrix of the spring volumes.

3 ELASTIC RESPONSE

3.1 Model elastic parameters

The spring elastic moduli $k^{(b)}$ are obtained imposing the equivalence of the stored strain energy over the fundamental cell volume between the RBSM and the continuum, for any strain state. For an isotropic Cauchy material it is reasonable to assume that the properties of the normal and shear springs (k^n, k^s) are independent from their side orientation. Instead, a different modulus k^d is considered for the diagonal

springs. Expressing the average spring strain in function of the strain tensor components for a generic homogeneous deformation state and considering the spring strain energies (Eq. 2), the total strain energy associated to the fundamental cell for square rigid elements $2l$ wide and s thick is the following:

$$\begin{aligned} U_{RBSMd} = & \frac{1}{2} s \Bigg[2k^n \varepsilon_{11}^2 2l^2 + 2k^n \varepsilon_{22}^2 2l^2 + \frac{1}{2} 4k^s \varepsilon_{12}^2 4l^2 + \\ & k^d \left(\frac{\varepsilon_{11} + \varepsilon_{22}}{2} + \varepsilon_{12} \right)^2 2l^2 + k^d \left(\frac{\varepsilon_{11} + \varepsilon_{22}}{2} - \varepsilon_{12} \right)^2 2l^2 \Bigg] \end{aligned} \tag{4}$$

Instead,according to the continuum Cauchy theory, for a plane stress state the strain energy stored in a volume equal to the fundamental cell one, for an isotropic material, is the following:

$$U_{continuum} = \frac{1}{2} 4l^2 s \left(\frac{E}{1-\nu^2} \varepsilon_{11}^2 + \frac{E}{1-\nu^2} \varepsilon_{22}^2 + \frac{2\nu E}{1-\nu^2} \varepsilon_{11} \varepsilon_{22} + 4 \frac{E}{2(1+\nu)} \varepsilon_{12}^2 \right) \tag{5}$$

The two energies are equal for any strain state if, and only if, the quantities that multiplies the different strain components are equal. In this way, the moduli of the model springs are obtained in function of the Young's modulus E and of the Poisson's ratio ν:

$$k^n = \frac{E}{1+\nu} \qquad k^d = \frac{4\nu E}{1-\nu^2} \qquad k^s = \frac{1-3\nu}{1-\nu^2} E \tag{6}$$

From the spring moduli expressions, it is evident the role of the diagonal springs, whose modulus is proportional to the Poisson's ratio, in agreement with a simple mechanistic structure of the model, that characterized the original model. But, differently from the original model there is not any constrain on the Poisson's coefficient. Anyway, for values of the Poisson's ratio lower than 0 or bigger than $1/3$ the diagonal spring modulus or the shear one, respectively, become negative, that seems nonphysical.
Considering the original RBSM (RBSMc), i.e. without the diagonal springs, in the RBSM strain energy there is not any term that multiplies $\varepsilon_{11}\varepsilon_{22}$ (Eq. 3.1). Therefore, even if the model has two spring modulus (Eq. 8), the response is anisotropic if the shear modulus G is different from $E/2$, i.e. if the Poisson's coefficient is not null, as previously introduced.

$$U_{RBSMc} = \frac{1}{2} s \left[2k^n \varepsilon_{11}^2 2l^2 + 2k^n \varepsilon_{22}^2 2l^2 + \frac{1}{2} 4k^s \varepsilon_{12}^2 4l^2 + \right] \tag{7}$$

$$k^n = \frac{E}{1-\nu^2} \qquad k^s = 2G = \frac{E}{1+\nu} \tag{8}$$

3.2 Elastic analyses

The proposed model is here validated comparing the results with a finite element model (FEM) for an uniaxial traction. A square lamina 1.5 m wide and 0.1 m thick was considered and a distributed volume load was applied on the edges over an area 0.1 m wide (Figures 2). For both the RBSM and the FEM it was adopted a similar discretization with square elements 0.1 m wide. About the material properties, the Young's modulus was assigned equal to 1.0 GPa and the Poisson's coefficient was varied between -1 and 0.5. Figure 3 shows the results for $\nu = 1/3$. The RBSM well reproduces the FEM results, with a limited error. The Poisson's coefficient estimated as the ratio between the displacements of the points R and

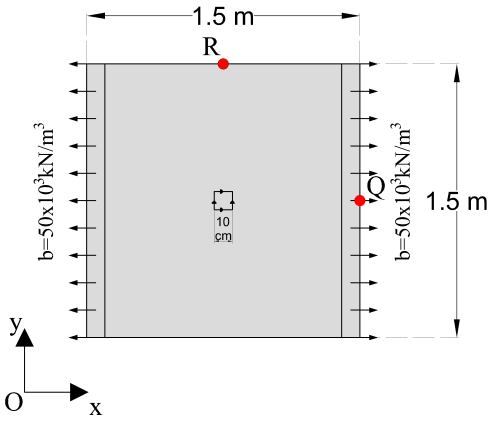

Figure 2: Geometry of the lamina for the elastic simple traction

Q (see Figure 2) is 0.336, with an acceptable error less than 1%. Figure 4 shows that also for negative Poisson's ratio, the model well reproduces the FEM results, even if the diagonal spring modulus is negative. The numerical estimated Poisson is -0.501 in this case, with an error of the 0.2%. Instead, it was observed that for Poisson's ratio bigger than 1/3 some numerical issues arise and the results are disturbed.

4 FAILURE RESPONSE

The addition of the diagonal springs increases the directions of the model in which the failure condition is checked, and this, according to the literature, should reduce the intrinsic failure anisotropy of the model. To evaluate this, the failure surface for a simple extension was computed estimating for any direction the minimum strain (ε_{Tf}) necessary to reach the failure condition in at least one spring. For this study, it was assumed the same failure average spring strain for both the normal and the diagonal springs, equal to the material elastic limit strain (ε_E). These springs fail according to a maximum stretch criterion, i.e. they fail if the average spring strain $\epsilon^{(b)}$ becomes bigger than the failure value ε_E. Instead, the shear springs fail only if the associated normal spring fails. The calculus was conducted for both the RBSM with and without the diagonal springs.
Figure 5 shows how the addition of the diagonal springs reduces significantly the failure anisotropy, as expected. The maximum error reduces from 100% to 20% for a simple extension, with a maximum stretch failure criterion.
If, on one hand, the addition of the diagonal springs reduces the failure anisotropy, on the other hand, the uni-axial response of the model in the side directions does not depend more only on the normal springs in that directions, but, the response of the normal and diagonal springs is coupled. For this reason, the spring behavior can not be directly related to the uni-axial material response. Furthermore, in order to study the failure response of brittle, or quasi-brittle materials, the fracture energy is not preserved assigning to the springs a perfectly brittle behavior with the failure strain equal to the material failure strain [20]. In order to eliminate the influence of the element size on the post elastic response, different strategies are possible: calibrate the spring failure strain on the mode I fracture energy, as it is usually done in peridynamics [16]; define a softening branch for the spring constitutive behavior, always based on the material fracture energy [17]. The softening branch can be linear or bi-linear, distinguishing an

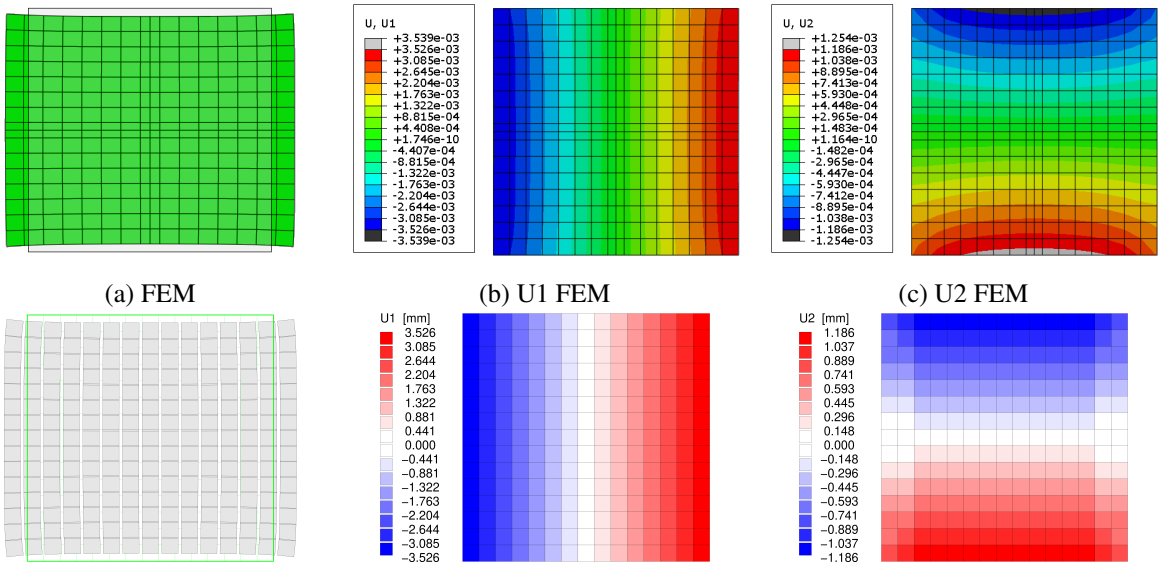

(a) FEM (b) U1 FEM (c) U2 FEM

(d) RBSMd (e) U1 RBSMd (f) U2 RBSMd

Figure 3: Comparison of the deformed shapes and of the displacement maps for a simple traction with $\nu = 0.333$

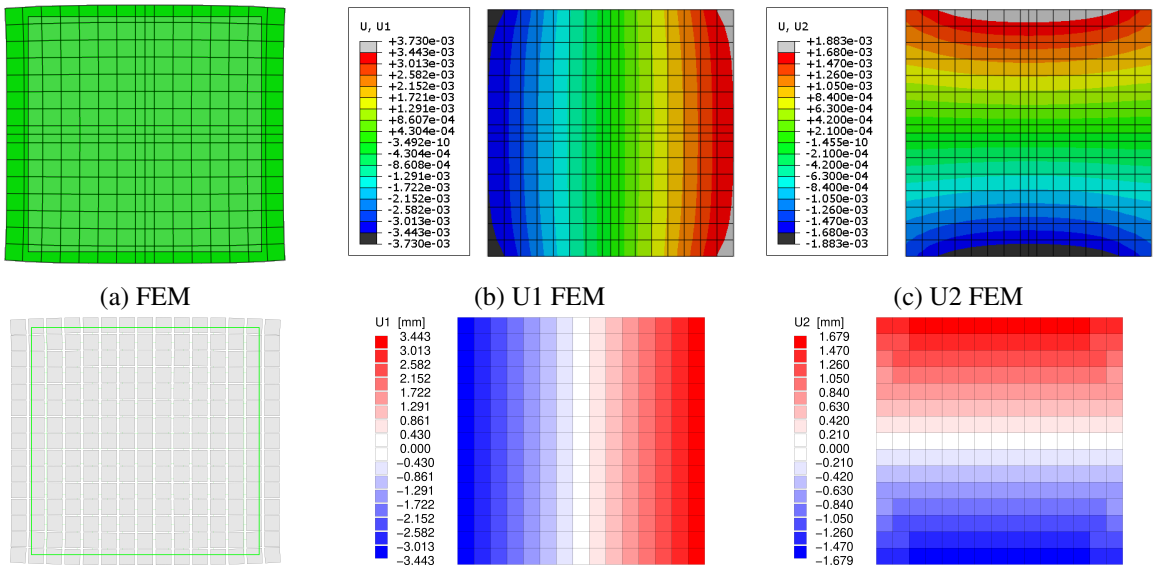

(a) FEM (b) U1 FEM (c) U2 FEM

(d) RBSM (e) U1 RBSM (f) U2 RBSM

Figure 4: Comparison of the deformed shapes and of the displacement maps for a simple traction with $\nu = -0.5$

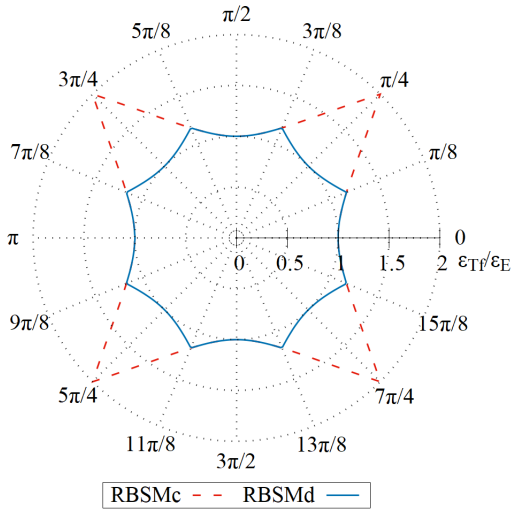

Figure 5: Comparison of the failure surfaces for a simple extension, obtained for the original RBSM (RBSMc) and the new one with the diagonal springs (RBSMd)

initial fracture energy G_f from the total fracture energy G_F. This is particularly important dealing with quasi-brittle materials (figure 6).
The spring constitutive behavior is defined assigning a spring force-average spring strain curve. The spring force $f^{(b)}$ is the quantity work conjugate of the average spring strain, it has the dimensions of a force multiplied for a length and coherently with the spring energy (Eq. 2) for the elastic case it is equal to:

$$f^{(b)} = \epsilon^{(b)}\, k^{(b)} V^{(b)} \tag{9}$$

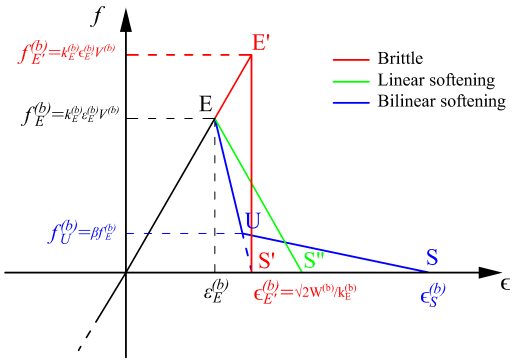

Figure 6: Example of $f^{(b)}$-$\epsilon^{(b)}$ relations for the model springs.

Table 1: Concrete mean mechanical properties

Young Modulus E (MPa)	37000
Poisson ratio ν	0.21
Tensile strength f_T (MPa)	3.9
Initial fracture energy G_f (N/m)	42.6
Total fracture energy G_F (N/m)	-

5 FAILURE ANALYSIS

5.1 Case study

For the failure analyses it was considered the experimental campaign, conducted by Grégoire et al. [10] with three point bending tests on concrete notched beams. More in detail, the beam considered for the analyses is 400 mm height and 50 mm thick with a central notch 80 mm deep (Figure 7). The concrete material properties are reported in Table 1. Considering that the article only refers to the initial fracture energy, the total concrete fracture energy was assumed equal to 2.5 times the initial value, considering the average ratio between these values for concrete [1].

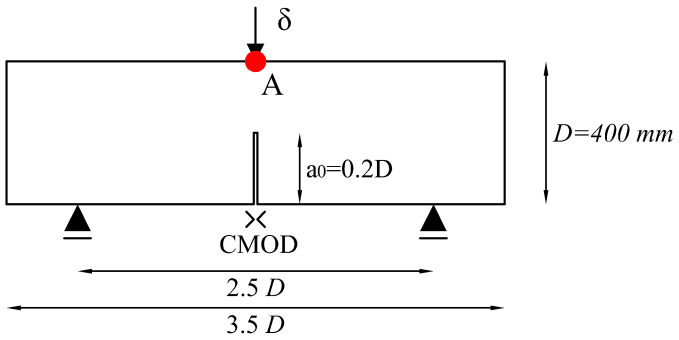

Figure 7: Geometry of the notched concrete beam

5.2 Numerical model

The beam was discretized in 5600 square elements 10 mm wide. About the failure behavior, an unlimited compressive strength was assigned to the normal and diagonal springs. About the tensile response, the analysis has been repeated changing 3 different behaviors (Figure 6). Instead, the shear springs only fail if the coupled normal spring fails. The different tensile curves (Tables 2-3) have been obtained in function of the material mode I fracture energy, imposing this equal to the model fracture energy for mode I along the element sides, i.e. the work necessary to breaks the springs interested by the crack propagation. For the laws with a softening branch, the elastic limit average spring strain was imposed equal to the material one.

The non linear analyses have been executed with an homemade FORTRAN code with an implemented explicit algorithm based on the central difference method. To limit the dynamic effects the displacement in the point A was increased up to 0.4 mm, with a cosine function, over a lapse of time of 0.2 s, decisively bigger than the higher problem vibration period (0.002 s). Furthermore, for stability reasons the

Table 2: Spring $f^{(b)}$-$\epsilon^{(b)}$ curve points for the spring tensile response with brittle and a linear softening laws.

Points	Brittle				Linear softening			
	Normal springs		Diagonal springs		Normal springs		Diagonal springs	
	$\epsilon^{(b)} \times 10^3$	$f^{(b)}$ (N·m)	$\epsilon^{(b)} \times 10^3$	$f^{(b)}$ (N·m)	$\epsilon^{(b)} \times 10^3$	$f^{(b)}$ (N·m)	$\epsilon^{(b)} \times 10^3$	$f^{(b)}$ (N·m)
E	0.478	36.58	0.656	53.34	0.105	8.06	0.105	8.57
S	0.479	0.00	0.657	0.00	2.17	0.00	4.09	0.00

Table 3: Spring $f^{(b)}$-$\epsilon^{(b)}$ curve points for the spring tensile response with a bi-linear softening.

Points	Bi-linear softening			
	Normal springs		Diagonal springs	
	$\epsilon^{(b)} \times 10^3$	$f^{(b)}$ (N·m)	$\epsilon^{(b)} \times 10^3$	$f^{(b)}$ (N·m)
E	0.105	8.06	0.105	8.57
U	0.648	2.42	1.190	2.57
S	5.290	0.000	9.940	0.000

time step was fixed equal to 1×10^{-7}

5.3 Results

In this simple I mode crack propagation problem the crack always propagates vertically from the notch, independently from the tensile behavior assigned to the springs (Figure 8), even if for the same displacement the corresponding crack opening displacement (CMOD) and consequently the crack propagation is different (Figure 9). In fact, the response curves change significantly. Comparing the force - crack mouth opening displacement (CMOD) curves, for the different tensile behaviors, with the experimental envelope (Figure 9b), it is evident that the brittle law significantly overestimates the peak load, with an error bigger than the 100%. The difference in shape is even more evident considering the force-displacement curve (Figure 9a), with a sudden load drop that is not realistic for concrete. Instead, for both the bi-linear and linear softening laws the F-CMOD curves are inside the experimental envelope, but for the bi-linear softening law the curve shape is more similar to the experimental one.

6 CONCLUSIONS

In this study the influence of the addition of the diagonal springs in a plane quadrilateral RBSM was investigated. First of all, it was proved that the addition of this new interactions extends the range of the isotropic materials that is possible to model with this discrete approach, at least in the elastic field. In fact, the proposed model eliminates the constrain of an intrinsic Poisson ratio. Anyway, for a Poisson ratio bigger than 1/3 some numerical issues arise, because the shear spring modulus become negative.
About the failure response, the addition of a new interaction in a new direction allows to significantly

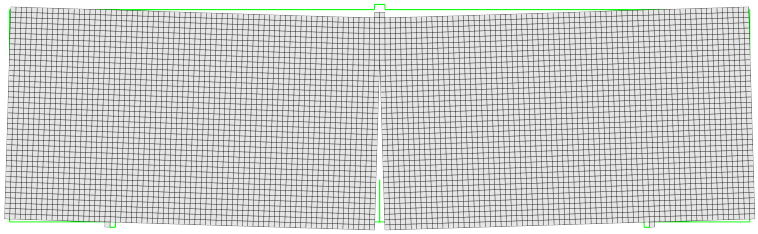

Figure 8: Deformed shape for $\delta = 0.4mm$ for the case with the bi-linear softening law

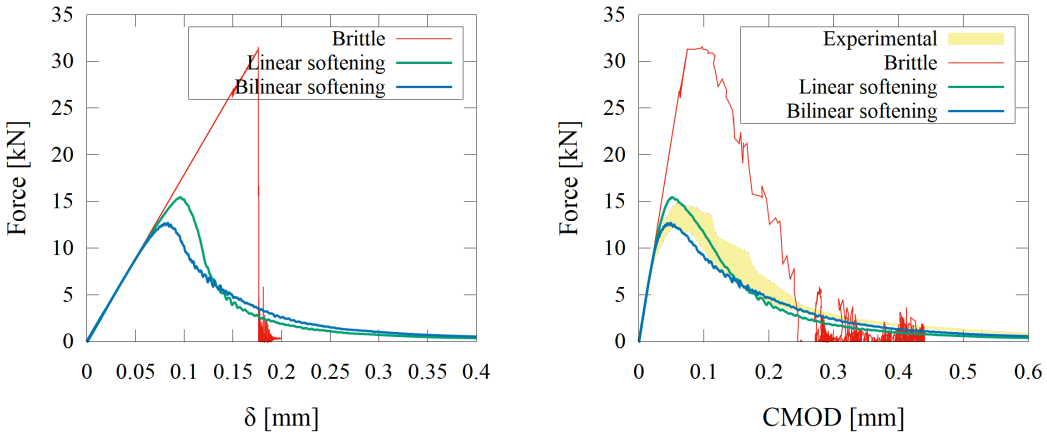

(a) F-δ

(b) F-CMOD

Figure 9: Comparison of the response curves obtained changing the spring tensile behavior.

reduce the failure anisotropy, in agreement with what has been observed for other discrete models. On the other hand, even if the model preserve a simple mechanicistic structure like the original one, the coupling between the diagonal springs and the normal one, for an uni-axial traction aligned with the rigid element sides, prevents to directly relate the spring behavior to the material uni-axial response. For this reason the fracture energy for mode I of the model was evaluated and set equal to the material one to obtain the spring tensile responses. This also avoids a mesh sensitivity of the results.
The proposed model was applied, in the end, to the analysis of a concrete notched beam in a three point bending test. Fixed the fracture energy assigned to the springs, the spring tensile behavior was changed between brittle, with a linear softening and a bi-linear softening branch. The last case provided the results closer to the experimental one, proving that in this discrete model, like in cohesive models the tensile response for modeling concrete has to have a bi-linear softening law.

REFERENCES

[1] Z. Bažant. Concrete fracture models: Testing and practice. *Engineering Fracture Mechanics*, 69(2):165–205, 2001. cited By 317.

[2] J. Bolander and S. Saito. Fracture analyses using spring networks with random geometry. *Engi-*

neering Fracture Mechanics, 61(5):569 – 591, 1998.

[3] D. Capecchi and G. Ruta. Strength of materials and theory of elasticity in 19th century italy: A brief account of the history of mechanics of solids and structures. *Advanced Structured Materials*, 52, 2015.

[4] S. Casolo. Modelling in-plane micro-structure of masonry walls by rigid elements. *International Journal of Solids and Structures*, 41(13):3625–3641, 2004.

[5] S. Casolo and V. Diana. Modelling laminated glass beam failure via stochastic rigid body-spring model and bond-based peridynamics. *Engineering Fracture Mechanics*, 190:331–346, 2018.

[6] S. Casolo, G. Milani, G. Uva, and C. Alessandri. Comparative seismic vulnerability analysis on ten masonry towers in the coastal po valley in italy. *Engineering Structures*, 49:465–490, 2013.

[7] S. Casolo and F. Peña. Rigid element model for in-plane dynamics of masonry walls considering hysteretic behaviour and damage. *Earthquake Engineering and Structural Dynamics*, 36(8):1029–1048, 2007.

[8] G. Cusatis, Z. P. Bažant, and L. Cedolin. Confinement-shear lattice csl model for fracture propagation in concrete. *Computer Methods in Applied Mechanics and Engineering*, 195(52):7154 – 7171, 2006. Computational Modelling of Concrete.

[9] V. Diana and S. Casolo. A bond-based micropolar peridynamic model with shear deformability: Elasticity, failure properties and initial yield domains. *International Journal of Solids and Structures*, 160:201 – 231, 2019.

[10] D. Gregoire, L. Rojas-Solano, and G. Pijaudier-Cabot. Failure and size effect for notched and unnotched concrete beams. *International Journal for Numerical and Analytical Methods in Geomechanics*, 37(10):1434–1452, 2013.

[11] A. Hrennikoff. Solution of problems of elasticity by the framework method. pages 169–175, 1941.

[12] L. Monette and M. P. Anderson. Elastic and fracture properties of the two-dimensional triangular and square lattices. *Modelling and Simulation in Materials Science and Engineering*, 2(1):53–66, 1994.

[13] M. Ostoja-Starzewski. Lattice models in micromechanics. *Applied Mechanics Reviews*, 55(1):35, 2002.

[14] Z. Pan, R. Ma, D. Wang, and A. Chen. A review of lattice type model in fracture mechanics: theory, applications, and perspectives. *Engineering Fracture Mechanics*, 190:382–409, 2018.

[15] S. Silling. Reformulation of elasticity theory for discontinuities and long-range forces. *Journal of the Mechanics and Physics of Solids*, 48(1):175–209, 2000.

[16] S. Silling and E. Askari. A meshfree method based on the peridynamic model of solid mechanics. *Computers & Structures*, 83(17):1526 – 1535, 2005. Advances in Meshfree Methods.

[17] Y. Tong, W. Shen, J. Shao, and J. Chen. A new bond model in peridynamics theory for progressive failure in cohesive brittle materials. *Engineering Fracture Mechanics*, 223:106767, 2020.

[18] G. Uva, V. Tateo, and S. Casolo. Presentation and validation of a specific rbsm approach for the meso-scale modelling of in-plane masonry-infills in rc frames. *International Journal of Masonry*

Research and Innovation, 5(3):366–395, 2020.

[19] G. Wang, A. Al-Ostaz, A. H. Cheng, and P. R. Mantena. Hybrid lattice particle modeling: Theoretical considerations for a 2D elastic spring network for dynamic fracture simulations. *Computational Materials Science*, 44(4):1126–1134, 2009.

[20] Z. Zhang, J. Ding, A. Ghassemi, and X. Ge. A hyperelastic-bilinear potential for lattice model with fracture energy conservation. *Engineering Fracture Mechanics*, 142:220–235, 2015.